Graphene-based nanomaterials for drug and/or gene delivery, bioimaging, and tissue engineering

Hong Zhao[1,2,‡], Ruihua Ding[1,3,‡], Xin Zhao[4], Yiwei Li[1,5], Liangliang Qu[1], Hao Pei[1], Lara Yildirimer[6], Zhengwei Wu[1,7] and Weixia Zhang[1]

[1] John A. Paulson School of Engineering and Applied Sciences, Harvard University, Cambridge, MA 02138, USA
[2] Research Institute of Petroleum Processing, SINOPEC, Beijing 100083, China
[3] Department of Chemistry and Chemical Biology, Harvard University, Cambridge, MA 02138, USA
[4] Interdisciplinary Division of Biomedical Engineering, the Hong Kong Polytechnic University, Hung Hom, Kowloon, Hong Kong, China
[5] Department of Mechanical Engineering, Massachusetts Institute of Technology, Cambridge, MA 02139, USA
[6] Barnet General Hospital Royal Free NHS Trust Hospital, Wellhouse Lane, Barnet EN5 3DJ, UK
[7] Department of Biomedical Engineering and Biotechnology, University of Massachusetts Lowell, Lowell, MA 01854, USA

Here, we discuss the biomedical applications of graphene-based nanomaterials (GBNs). We examine graphene and its various derivatives, including graphene, graphene oxides (GOs), reduced graphene oxides (rGOs), graphene quantum dots (GQDs), and graphene composites, and discuss their unique properties related to their biomedical applications. We also summarize the detailed biomedical applications of GBNs, including drug and/or gene delivery, bioimaging, and tissue engineering. We also highlight the toxicity of these nanomaterials.

Introduction

Since its unexpected discovery in 2004 [1,2], graphene has been propelled to the forefront of technological advancement with an almost infinite list of applications, for example, future electronics [3,4], energy or hydrogen storage [5,6], and biosensing [7,8], as result of its unique electronic, optical, thermal, and mechanical properties [9–12]. Graphene derives its properties from its chemical structure, which comprises a flat monolayer of carbon atoms packed into a 2D honeycomb lattice; this lattice is a basic building block for all other graphitic materials (Fig. 1).

Such versatility, combined with electronic flexibility [4,13], a large surface area [14], high mechanical strength [15], high intrinsic mobility [16,17], and unparalleled thermal conductivity [11], have rendered graphene and graphene-based materials attractive as technological tools. However, it was not until 2008 that graphene-based materials were first introduced into the field of biomedical sciences, when Dai et al. used GO as an efficient nanocarrier for drug delivery [18]. Since then, interest in its biomedical applications has gained momentum, from drug and/or gene

Corresponding author: Zhang, W. (wxzhang@seas.harvard.edu)
‡ These authors contributed equally to this article.

Hong Zhao received her BSc in chemical engineering from Sichuan University, Sichuan, in 2011 and her PhD from Tsinghua University, Beijing, China in 2016. She attended Harvard University as a visiting student under the supervision of David Weitz in 2014. Hong is currently an engineer in the Research Institute of Petroleum Processing (RIPP), Sinopec. Her research interests include nanocomposites, bioenergy, tracers, additives, and separation and purification processes.

Ruihua Ding received his BSc from the University of Wisconsin-Madison. He is currently a graduate student at Harvard University. His current research interests focus on the interface between biology and materials science, and on accessing and manipulating cell behaviors using nanomaterials and microstructures.

Weixia Zhang received his MSc in chemistry from Tsinghua University in 2008 and his PhD in chemistry from Purdue University in 2014. Following his PhD, he joined the John A. Paulson School of Engineering and Applied Sciences at Harvard University, where he is currently a Research Associate. His research interests span a wide range of topics in Chemistry and Materials Sciences, including organic synthesis, self-assembly, surface chemistry, the design and synthesis of various functional nanomaterials (including mesoporous materials; and carbon nanomaterials, such as graphene, and silicon nanowires), and biomedical applications of nanomaterials, and microfluidics.

http://dx.doi.org/10.1016/j.drudis.2017.04.002

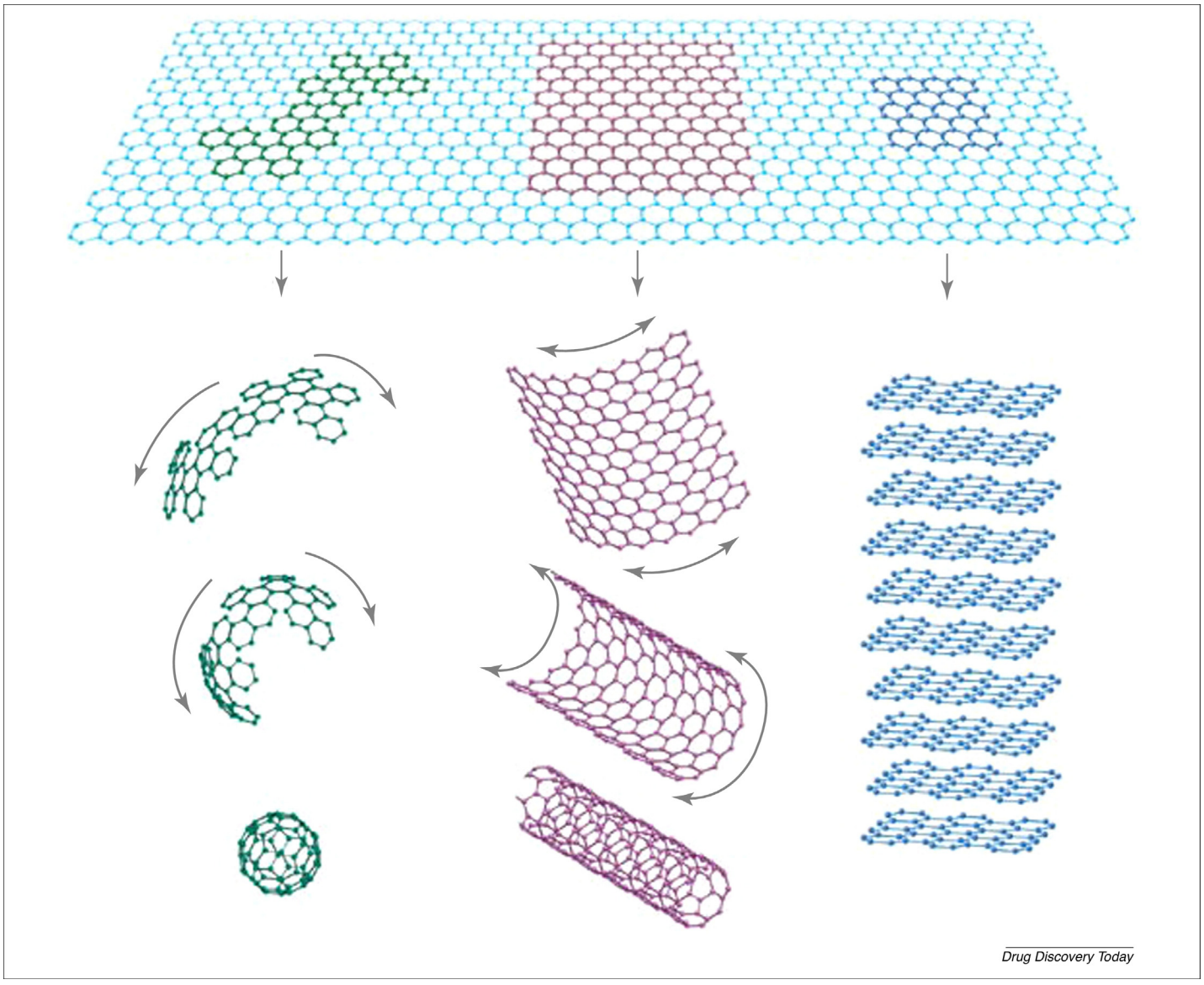

FIGURE 1

Graphene as a 2D building material for carbon materials of all other dimensionalities, including 0D bucky balls, rolled 1D nanotubes, or stacked 3D graphite. Adapted, with permission, from Ref. [4].

delivery, to bioimaging, and biomedical devices for tissue engineering. Given their ability to interact with biomolecules, such as DNA, and protect them from enzymatic degradation, as well as their capacity to act as delivery vehicles in living cells and *in vivo* systems, graphene and its derivatives have firmly established themselves as next-generation candidates for biotechnological advancements. Therefore, here, we summarize and critically appraise developments at the interface of graphene-based materials and biomedical science. We focus specifically on the impact of graphene on novel drug and/or gene delivery, bioimaging, and tissue engineering. Furthermore, we discuss the anticorrosion property of graphene in terms of using graphene coatings for biomedical implants and devices. Although we do not discuss graphene synthesis or its chemical and physical properties, in-depth information can be found elsewhere in several excellent reviews [3,13,19–21]. Despite the enthusiasm and reasons to be excited about the role of graphene in the biomedical arena, important concerns regarding its biocompatibility and safety remain, and these are also discussed.

Graphene-based nanomaterials

GBNs include graphene derivatives and graphene-based composites. Graphene derivatives, such as GO, rGO, GQDs, or nano-reduced graphene oxide (nano-rGO), can be obtained by using graphene or graphite as the starting material [22]. These are distinguished from each other in terms of their surface properties, number of layers, and size (Fig. 2).

GO, an oxidation form of graphite, usually has single, bi- or multilayers of graphene sheets with epoxide, hydroxyl, and carboxylic acid groups [23]. GO is commonly synthesized using the Hummers method or derivatives thereof [24,25], which involves oxidation of graphite to various levels by using potassium permanganate and sulfuric acid. GO contains a range of oxygen functional groups, mainly hydroxyl and epoxy groups on the basal

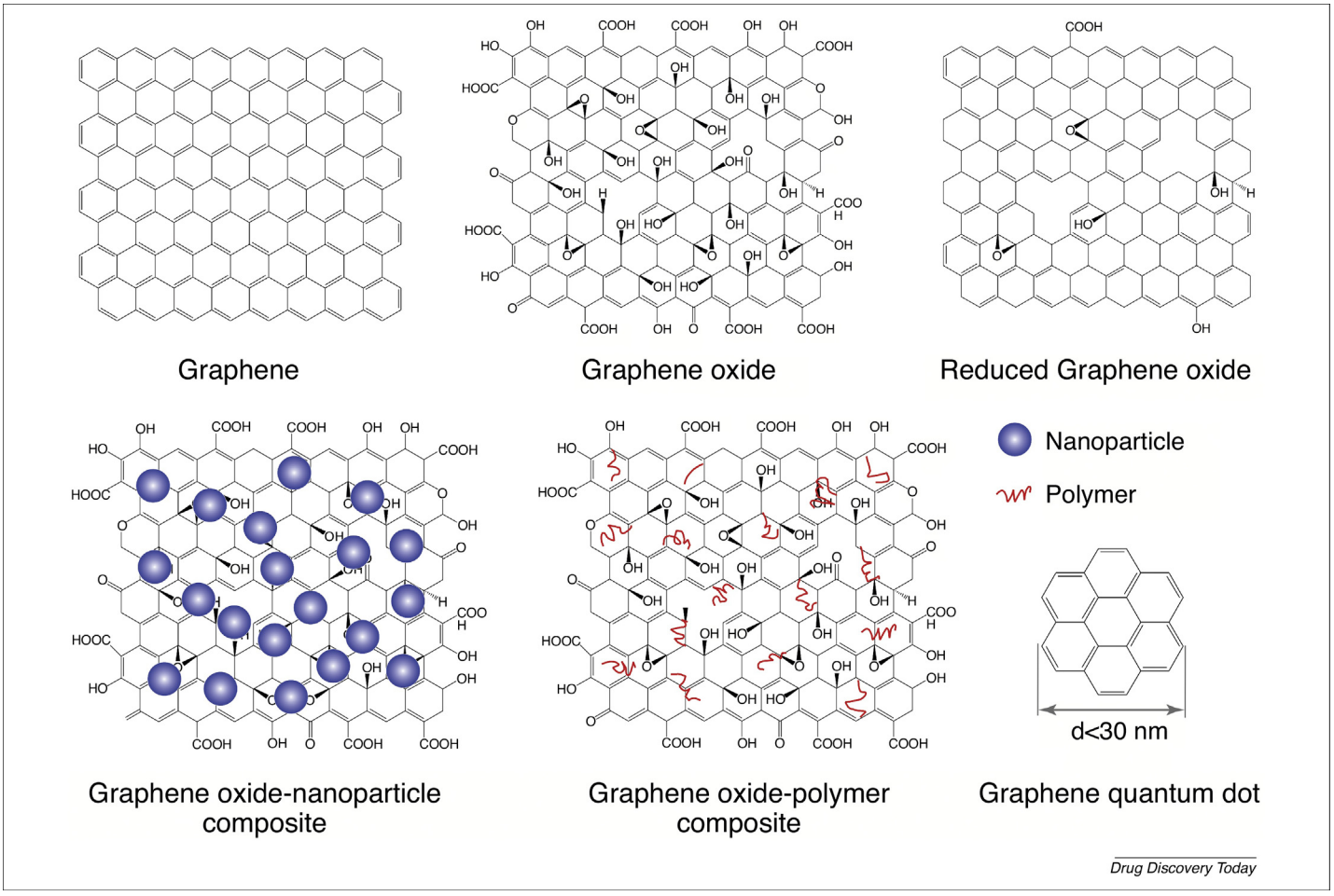

FIGURE 2

Schematic illustration of different graphene-based nanomaterials.

plane, with smaller amounts of carboxyl, carbonyl, phenol, and lactone at the sheet edges [21,26–29]. The hydroxyl and epoxy groups form hydrogen bonds and weak interactions with other groups, whereas the carboxylic acid group offers negative surface charge and stability in polar solutions. Thus GO disperses well in water and other polar solvents [30]. In addition, GO is also amphiphilic, acting as a surfactant because of the hydrophobic properties of free surface π electrons from the unmodified graphene. More importantly, these reactive oxygen functional groups of GO enable researchers to conduct further chemical functionalizations to render GO an ideal platform for the accommodation of biomolecules, which is a key factor for its bio-related applications [26,31]. Even though the reactive oxygen functional groups increase the stability of graphene in solution as well as its chemical reactivity, the disrupted sp^2 decreases its mechanical, electrical, and thermal properties [23].

rGO is obtained by reducing GO to remove its oxygen functional groups [32]. Thermal and ultraviolet (UV) treatment of GO, or chemical treatment with hydrazine [33,34], ascorbic acid [35,36], sodium borohydride [37,38], hydroquinone [39,40] or other reducing agents [41–44] can restore the conjugated structure to form rGO. The recovered graphitic network of rGO results in a lower percolation threshold and fewer junctions, giving rise to its high electrical conductivity [45,46]. Although rGO has less oxygen content, surface charge, or hydrophilic functional groups compared with GO [23], it has been modified by noncovalent interactions, including π–π stacking and van der Waals interactions, to physically adsorb both polymers [47,48] and small molecules [49,50] onto its basal plane. Various studies have demonstrated that rGO is biocompatible, making it suitable for cell culture, biosensing, tissue engineering, and other biomedical applications [51–53].

GQDs or nano-rGOs represent single layers or more (up to ten layers) of graphene or rGOs of a lateral size less than 30 nm [54–56]. GQDs can be fabricated using both top-down and bottom-up approaches. Top-down approaches involve cutting large graphene sheets into ultrasmall GQDs using different physical, chemical, or electrochemical techniques, including hydrothermal process [57], chemical exfoliation [58], electrochemical oxidation [59], and electron beam lithography [60]. Bottom-up approaches refer to the synthesis of aromatic compounds as graphene moieties with a certain number of conjugated carbon atoms. Such approaches involve oxidative condensation reactions [61], pyrolysis [54,55], cage opening of fullerene [62], and nitration of pyrene [63]. As a result of strong quantum confinement and edge effects, GQDs show intense intrinsic photoluminescence, which can be further tuned by controlling their size, shape, defects, and functionalities [64–69]. Furthermore, compared with conventional

semiconductor quantum dots, which suffer from high toxicity induced by the heavy metals used, GQDs have many advantages, such as low toxicity and excellent biocompatibility [70,71]. Thus, GQDs have been widely used in biosensing [72], cellular imaging [73], drug delivery, and photodynamic therapy [74,75].

In addition to the above graphene derivatives, based on the surface π electrons and functional groups, such as –COOH, –COC–, and –OH, graphene-based materials can be functionalized with a large number of polymers, inorganic materials, and cells through covalent or noncovalent interactions to obtain specific properties or reduce their toxicity. Different graphene-based composites used commonly in biomedical applications are discussed below.

As a result of the variety of the active functional groups of carboxylic acid, epoxy, and hydroxyl groups, GO can be widely functionalized with organic materials to improve water stability and reduce toxicity for biomedical applications. Polyethylene glycol (PEG) is one of the most used polymers to modify GO for good water stability and biocompatibility [76–78]. PEGylated nano-graphene and GO are usually prepared by adding NH_2-PEG-NH_2, 1-ethyl-3-(3-dimethylaminopropyl)carbodiimide (EDC), and *N*-hydroxysuccinimide (NHS) to stabilize the nano-GO (nGO) solution, followed by mixing at room temperature for 2 h and then by centrifuging and washing [79]. Dextran has also been used to composite with nGO through π–π interactions to improve the physiological stability for better drug delivery. For example, Jin et al. synthesized nGO-dextran-hematin hybrids by mixing a nGO solution with dextran-hematin in water followed by a reaction with ammonia and hydrazine solution [80]. The resulting nGO-dextran-hematin hybrids exhibited better colloidal stability in serum and cytocompatibility. In addition, 4-arm polypropylene oxide (PPO)-polyethylene oxide (PEO)-tyramine (Tet-TA) [81], poly(vinyl alcohol) (PVA) [82], polyethylenimine (PEI) [83,84], chitosan [85,86], and amphiphilic copolymers [87] have also been used to improve the stability.

Graphene-based organic-inorganic hybrid materials are also widely used in the biomedical field for bioimaging, biosensing, and drug delivery. Solanki et al. encapsulated GO rich in oxygen groups on the surface of positively charged silica nanoparticles through electrostatic interaction [88]. The GO-Si hybrid NPs were obtained using GO nanosheet coating on the surface of silica NPs with diameter of 300 nm. Zhou et al. prepared GO/Au and GO/Ag composites in two steps. GO-CSH (cystamine dihydrochloride) were first prepared by adding CSH solution to the mixture of GO-COOH aqueous solution and MES solution with EDC followed by filtration and washing [89]. Then, the GO/Au and GO/Ag composites were obtained by mixing the prepared CO-CSH with noble metal NPs in water and stirred at 35 °C for 24 h. Chen et al. prepared Fe_2O_3@Au core@shell NP–rGO nanocomposites for bioimaging [90]. Amino-functionalized PEGylated Fe_2O_3@Au NPs and carboxylated rGO were first prepared. Then, an amino-functionalized PEGylated Fe_2O_3@Au NPs solution was added to the mixture of rGO-COOH, EDC, sulfo-NHS, and MES buffer, followed by stirring for 1 h. After treatment with NaOH, ultrasonication, and centrifuging, rGO-Fe_2O_3@Au NP nanocomposites were obtained. Other inorganic materials, such as manganese ferrite [91], ZnS [92], and hydroxyapatite (HA) [93], have been widely used to composite with graphene-based nanomaterials for biomedical applications.

Other graphene-based nanocomposites have also been prepared for improved biomedical applications. For example, graphene–cell biocomposites were prepared to extend the application of graphene-based nanomaterials beyond planar tissue cultures [94].

Other graphene-based nanocomposites and their fabrications, as well as their applications, are detailed in Table 1.

TABLE 1

Graphene-based nanocomposites and their fabrications as well as applications

Graphene-based nanocomposites	Fabrication	Applications	Refs
Trimethyl chitosan/GO	GO suspension mixed with folated conjugated trimethyl chitosan followed by sonication	DOX and gene delivery	[86]
rGO-HA	Hydroxyapatite microparticles suspension mixed with rGO suspension followed by being vortexed	Stimulating osteogenic differentiation of human MSC	[93]
GO-MSCs	GO cultured in the supplemented DMEM medium overnight followed by adding MSCs	Enhanced chondrogenic differentiation	[94]
(2-dimethylamino)ethyl methacrylate (DMAEMA)-GO	Surface-initiated ATRP of DMEAMA to GO-SS-Br	CPT delivery	[195]
PAMAM-graphene	Graphene alcohol suspension mixed with oleic acid followed by conjugating PAMAM via EDC-coupling reaction	Gene delivery	[121]
PLA-PEG-grafted GQDs	NH_2-PEG-NH_2 conjugated to the activated carboxyl GQDs via EDC-coupling followed by the 2nd EDC coupling to conjugate PLA	Gene delivery and cell imaging	[137]
Organosilane-GQDs	Organosilane in ethanol mixed with GO suspension under ultrasonic condition	Cell imaging	[138]
GO-polypeptide	GO suspended in the PEG-PA aqueous solution followed by changing temperature to form hydrogel composite	Adipogenic differentiation of tonsil-derived MSCs	[196]
Octaarginine-GO	Activation of GO with NHS followed by reacting with octaarginine	Gene delivery	[197]
GO-Manganese Ferrite (MF)	Oleylamine grafted GO mixed with MF NPs under ultrasonic condition	Hyperthermia agent	[91]
GO-ZnS	GO-PEG functionalized with reduced glutathione-coated ZnS nanocrystals via an amidation reaction	Drug delivery and cell labeling	[92]
NGO-PEG-Chlorin e6, NGO-branched polyethylenimine (BPEI)-Chlorin e6	Ce 6 conjugated to NGO-PEG or NGO-PEG-BPEI	Photodynamic therapy	[198]

Properties of graphene-based nanomaterials

Since being isolated in 2004, graphene has been intensively studied in terms of its fascinating properties. As a 2D material, graphene has a huge surface area that is approximately 2630 m^2/g [14]. The strong C–C covalent bonds within the graphene sheet render it one of the hardest materials, with a Young's modulus of 1100 GPa and a fracture strength of 130 GPa [15]. The π–π bonds below and above the atomic plane give graphene exceptional thermal and electrical conductivity. Single graphene has been reported to have a thermal conductivity of 5000 W/m/K [11]. The electrical conductivity of graphene has been reported to be 10000 S/cm [95], combined with ultra-high intrinsic mobility of 200 000 $cm^2v^{-1}s^{-1}$ [16,17]. More details about graphene properties can be found elsewhere [96,97]. Here, we mainly emphasize properties of graphene-based materials that are closely related to their biomedical applications.

The first unique feature of graphene-based materials is their 2D planar structure with a high specific surface area; this enables them to be loaded or to interact with various chemical compounds and biological species. For graphene, the free π electrons at a high density on its planar surface make it suitable for electrophilic reactions with several organic molecules, such as click reactions, cycloadditions, and carbine insertion reactions [98]. Meanwhile, the conjugated basal plane enables graphene to interact with many drugs or other biomolecules containing aromatic structures via π–π stacking to fabricate biosensors [99]. The hydrophobic nature of graphene can also be used to absorb various hydrophobic organic molecules or polymers via van der Waals interaction [100]. In terms of GO, rGO, and other graphene derivatives, in addition to the above noncovalent π–π stacking and van der Waals interactions, the abundant oxygen functional groups on these derivatives provide more ways in which to immobilize molecules or biomolecules through both noncovalent interactions, including hydrogen bonds and ionic interactions, and covalent bonds via chemical reactions. Oxygen-containing groups, mainly ionic carboxylates and hydroxylates, can participate in ionic interactions or hydrogen bonding with the analogous ionic parts of biomolecules to facilitate the loading of the latter, which can be used for drug or gene delivery applications [101–103].

The astonishing mechanical properties of graphene have also inspired researchers to fabricate graphene-based composites with enhanced mechanical strength for various biomedical applications. Graphene, as a reinforcing filler, can improve the mechanical properties of many soft materials, such as hydrogels or polymer films [104], when forming graphene-based composites. After being oxidized, although the damaged structure leads to compromised mechanical properties of GO and other derivatives, both GO and rGO have been explored for enhancing the mechanical strength of polymeric materials, including PVA and poly(methyl methacrylate) [105]. These reinforced composites with increased Young's modulus and hardness are suitable for tissue-engineering applications.

Graphene and rGO have excellent electrical conductivity that can be utilized to fabricate electrical biomedical devices, including field-effect transistor biosensors, and to act as a substrate for conductive cell culture devices [106–108]. The low electrical conductivity of GO, which results from structure defects, limits the direct applications of GO in electrically active materials and device;, however, the oxygenated functional groups of GO can be used to immobilize various electroactive species through covalent or noncovalent bonds to fabricate sensitive electrochemical systems [26]. In addition, the good dispersibility of GO in many polar solvents, particularly water [21,30,109], makes it easy to process GO. The stable GO suspension can be deposited on electrodes to form thin conductive films that act as active electrode materials that can be used to detect or sense many biomolecules, including DNA, enzymes, and proteins [26].

Finally, the optical properties of graphene-based materials are also useful for biomedical applications. Monolayer graphene has a light transmittance of 97.7% of the total incident light over a range of wavelengths [110]. Light absorption of graphene increases with its layer number [111]. When graphene size is reduced to the nanoscale to form nanoribbons, it can emit intrinsic photoluminescence because of band gaps that induced at this nanoscale. Similar properties are also observed in GO and GQDs, which enable researchers to apply these graphene-based materials for biomedical imaging [101,112]. In addition, GO has been demonstrated to be an efficient fluorescent quencher for a variety of fluorophores via nonradioactive electronic excitation energy transfer from the fluorophore to GO; this property has been exploited for biosensing, particularly as a fluorescence resonance energy transfer sensor, given its large adsorption cross-section [113–115]. Additionally, graphene and its derivatives have strong optical adsorption in the near-infrared range, making them powerful agents for photothermal therapy [116].

Biomedical applications of graphene-based nanomaterials

Drug delivery

Over the past few years, motivated by the successes of carbon nanotubes in biomedicine, functionalized graphene has been explored in drug delivery. The advantages of graphene-based nanomaterials for drug delivery arise from their ability to cross cell membranes easily and their high specific surface area, which provides multiple attachment sites for drug targeting. Graphene-based nanomaterials can load drugs noncovalently via π–π stacking interactions, hydrogen bonding, or hydrophobic interactions.

Initial studies using graphene-based nanomaterials for drug delivery were conducted by Dai et al. who loaded a camptothecin (CPT) analog, SN38 to GO-PEG via π–π stacking. The complex exhibited good water solubility, retaining a high efficiency of SN38 delivery, as well as high cytotoxicity in cells [18]. Inspired by this pioneer work, many researchers have published studies exploring graphene-based materials for drug delivery. For instance, the same group reported the targeted delivery of rituxan using GO-PEG [101]. Jin et al. prepared hematin-conjugated dextran-functionalized GO hybrids via π–π interactions to deliver doxorubicin (DOX) for killing drug-resistant MCF-7/ADR cells [80]. Improved physiological stability was obtained and this hybrid had a loading capacity as high as 3.4 mg/mg nGO. The authors demonstrated that the release profile was pH dependent, with more released at lower pH; approximately 30% of the DOX was released over 6 days and the DOX-loaded hybrids accumulated effectively in the cytoplasm and nucleus to kill the cells (Fig. 3a). A similar pH-dependent DOX release profile was obtained when GO-PEG/ZnS:Mn composites were used as carriers (Fig. 3bi) [92]. DOX was loaded

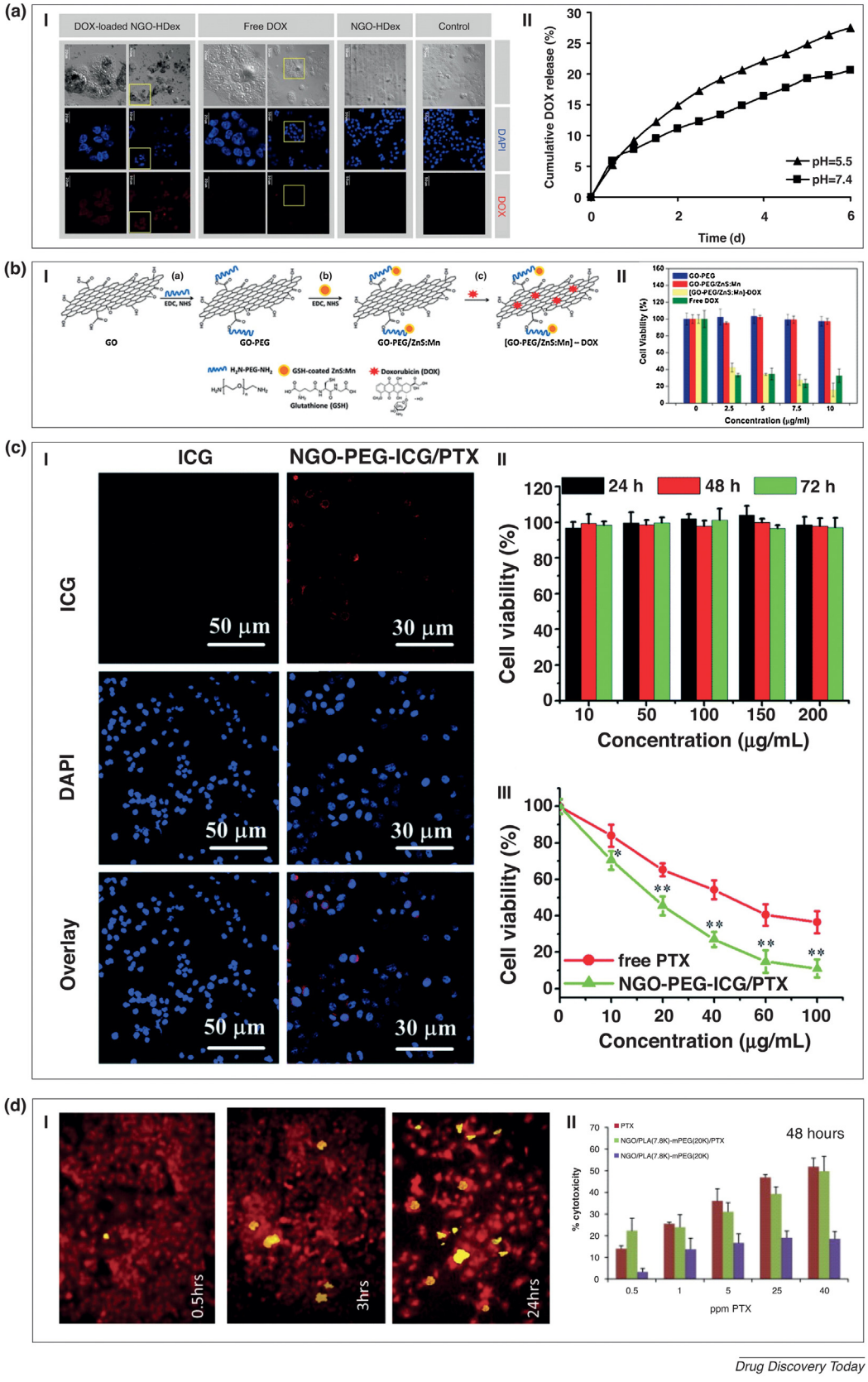

Drug Discovery Today

FIGURE 3

Graphene-based nanomaterials for drug delivery. (a) (i) Confocal laser microscopic observation of MCF-7/ADR cells after incubation with NGO — HDex1, free doxorubicin (DOX) or DOX-loaded NGO — HDex for 24 h. (ii) Cumulative DOX release from NGO — HDex1 as a function of time. (b) (i) Schematic illustration of the formation of [GO-PEG/ZnS:Mn]-DOX composites. (ii) Relative cell viability of HeLa cells incubated for 24 h with different concentrations of GO-PEG and GO-PEG/ZnS:Mn with and without DOX, and with free DOX. (c) (i) Cellular uptake of free ICG and NGO-PEG–ICG/PTX. (ii) The cytotoxicity of different concentrations of

TABLE 2

Other drugs delivered using graphene-based nanomaterials

Carriers	Drugs	Applications	Refs
nGO-PEG	Cisplatin	Inhibition of cell proliferation and morphology deformation	[199]
nGO-folic acid	DOX and camptothecin delivery	Targeted delivery of mixed anticancer drugs	[103]
PNIPAM-GS	Camptothecin	Temperature-dependent drug release with high CPT-loading efficiency	[200]
GO-PEG	Ce6 photosensitizer	Photodynamic therapy	[122]
Chitosan-GO	Ibuprofen, 5-fluorouracil	Controlled release of chemically diverse drugs	[201]
GN-CNT-Fe_3O_4	5-fluorouracil	pH-dependent drug release	[202]
GO	Hypocrellin	Photodynamic therapy	[203]

on the composite particles noncovalently and the loading capacity was dependent on the concentration of GO-PEG/ZnS:Mn, because more GO surface was available for DOX binding. When 1000 mg/ml of a GO-PEG/ZnS:Mn solution was mixed with 300 mg/ml of a DOX solution, the loading capacity reached 100%. The DOX-loaded composite particles killed approximately 85% of HeLa cancer cells (Fig. 3bii). To further control the drug release, PEGylated Fe_2O_3@Au core-shell NP-rGO nanocomposites were prepared to control the loaded DOX via synergistic interactions between photothermal therapy and chemotherapy [90]. The maximal DOX loading capacity was approximately 1.0 mg/mg nanocomposites via π–π stacking interactions. When the DOX-loaded composites were put in PBS of pH 7.4, 17% of DOX was released in 2 h, although a burst release occurred following irradiation under an 808-nm NIR laser. In addition, via magnetic field guidance, DOX–rGO–Fe2O3@Au NPs killed cells close to the magnetic field. Therefore, the loaded DOX could be released at specific sites and at a controlled rate. Zhou et al. also prepared graphene/Fe_3O_4composites using graphite oxide and $FeCl_3 \cdot 6H_2O$ as starting materials and used the composites to load DOX [117]. Given the the large specific surface area provided by graphene and the π–π interactions between graphene and DOX, a 65% loading capacity was obtained, which was higher than GO with the same Fe_3O_4. Meanwhile, the use of Fe_3O_4 NPs also led to better bioimaging because of the enhanced cell-to-background contrast [77].

In the delivery of paclitaxel (PTX), graphene-based nanomaterial-loaded PTX provided better cytotoxicity against cancer cells. Xu et al. functionalized GO with PEG to improve its stability in a physiological solution [118] and then loaded PTX onto the GO-PEG composites via π–π stacking and hydrophobic interactions, resulting in a relatively high loading capacity of 11.2 wt%. In a cellular uptake experiment, GO-PEG/PTX entered A549 and MCF-7 cells within 1 h. Compared with free PTX, GO-PEG/PTX of same amount led to lower cell viability, with an approximately 30% and 10% relative cell viability of A549 and MCF-7, respectively. Similar results were also obtained by Zhang and colleagues using PEGylated nGO to co-deliver PTX and indocyanine green (ICG) [79]. Low cytotoxicity was observed of nGO-PEG on MG-63 cells even at a concentration of 200 mg/m. Meanwhile, lower cell viability was obtained with nGO-PEG-ICG/PTX compared with free PTX (Fig. 3c). Angelopoulou et al. modified GO with poly (lactide)–poly(ethylene glycol) (PLA–PEG) copolymers for stability in an aqueous solution [119]. The PTX release profile was regulated by the molecular weight of PLA or PEG in the copolymer and their proportion in the composite, with a smaller molecular weight and larger proportion leading to faster release. The PTX-loaded composites demonstrated cytotoxicity against A549 cells with an increasing incubation time (Fig. 3d).

Other drugs have also been delivered using graphene-based nanomaterials in addition to those described above, and selected examples are detailed in Table 2.

Gene delivery

Gene therapy is a technique that uses genes to treat a genetic disease, and this approach has attracted intensive research attention. A key factor for gene therapy is to find efficient and safe gene vectors that protect DNA from nuclease degradation and facilitate its uptake with high transfection efficiency [23,120]. Graphene-based nanomaterials are appropriate candidates for gene delivery because of their high loading efficiency and increased gene transfection. To decrease their cytotoxicity and obtain cationic surface properties to allow their interaction with anionic oligonucleotides electrostatically, graphene derivatives have to be modified by polymers, such as chitosan [86], polyamidoamine (PAMAM) [121], polyethylenimine (PEI) [83], and so on. Zhang et al. reported using PEI-conjugated GO to sequentially deliver siRNA and DOX [122], exhibiting a synergistic effect that led to significantly improved therapy efficacy. Liu et al. explored using PEI-functionalized GO for gene delivery using different molecular weights of PEI [123], and showed significantly low cytotoxicity of the PEI-GO complex and successful use of GO as a novel nano-gene delivery vector with high transfection efficiency. Lactosylated chitosan oligosaccharide (LCO)-functionalized graphene oxides (GO-LCO) was prepared for the targeted delivery of DNA sequences to human hepatic carcinoma cells (QGY-7703) [85]. The loading capacity of FAM-DNA was as high as 4 mmol/g and it was delivered specifically to QGY-7703 within 0.5 h. In addition, no obvious toxicity was observed even at concentration of 100 mg/m. Hu et al. prepared folate-conjugated trimethyl chitosan (FTMC)/GO nanocomplexes (FG NCs) via electrostatic self-assembly to realize the targeted delivery of plasmid DNA (pDNA) [86]. Compared with A549 cells, Hela cells with folate receptors exhibited higher accu-

NGO-PEG on MG-63 cells at various treatment times. (iii) The cytotoxicity of different concentrations of free paclitaxel (PTX) and NGO-PEG–ICG/PTX (at the same concentration of PTX) on MG-63 cells. (d) (i) Fluorescence microscopy images of NGO/PLA(7.8 K)–mPEG20 K composite uptake by A549 cells. Cells were incubated for different times (h) with FITC-labeled composites. PI was used to stain the nuclear and cytoplasmic nucleic acids red after incubation and overlay images are shown (magnification 20 x). (ii) Cytotoxicity of blank NGO/PLA (7.8 K)-mPEG(20 K) composites, PTX-loaded NGO/PLA(7.8 K)-mPEG(20 K) composites, and PTX against A549 cancer cells. Adapted, with permission, from [80] (a), [92] (b), [79] (c), and [119] (d).

mulation of FG NCs. The existence of FTMC in FG NCs could retard the migration of pDNA and facilitate pDNA condensation. It was reported that 31.1% of pDNA could be released within 72 h *in vitro* in PBS, highlighting FG NCs as a promising candidate for gene delivery. Liu et al. synthesized graphene-oleate-PAMAM dendrimer hybrids via oleic acid adsorption followed by covalent linkage of PAMAM dendrimers as gene delivery vectors [121]. The graphene-oleate-PAMAM exhibited good dispersity in aqueous solutions and good biocompatibility with HeLa cells, but showed cytotoxicity to MG-63 cells at concentrations >20 mg/ml. The graphene-oleate-PAMAM loaded with a quarter of pEGFP-N1 exhibited a GFP gene transfection efficiency of 18.3% to HeLa cells (Fig. 4ai,ii). PAMAM dendrimer-grafted gadolinium-functionalized GO [124] and mPEGylated GO/poly(2-dimethylaminoethyl methacrylate)(PDMAEMA) nanohybrids [125] were also synthesized for RNA delivery to obtain improved gene transfection efficiency and good biocompatibility. Teimouri et al. prepared three different GO-based nanocarriers for gene delivery based on the conjugation of GO with cationic polymers of PEI, polypropylenimine (PPI), and PAMAM to compare their cytotoxicity and transfection efficiency [83]. GFP was used to evaluate the transfection efficiency and the results showed that PEI-GO conjugate was ninefold more effective in the EGFP-transfected cells. Choi et al. also prepared GO-PEI complexes to effectively load mRNA for clinical applications [84] (Fig. 4b). After treatment with GO-PEI/RNA complexes, the cells increased their reprogramming efficiency and rat and human induced pluripotent stem cells (iPSCs) were generated successfully from adult adipose tissue-derived fibroblasts without repetitive daily transfection.

In addition to DNA, proteins can also be delivered using graphene-based materials for gene therapy. Zhang et al. reported the co-delivery of ribonuclease A and protein kinase A to the cell cytoplasm without enzymatic hydrolysis and loss of biological activity intracellularly, by loading proteins onto GO-PEG with a high payload via noncovalent interactions [126]. Hong and coworkers used multilayer GO-poly (β-amino ester) to entrap ovalbumin (OVA), a protein antigen [127], and demonstrated that the multilayer films blocked the initial burst release of OVA and could be precisely controlled to trigger its release upon the application of electrochemical potentials. Other examples include loading bone morphogenic protein-2 (BMP-2) to a GO-coated Ti substrate to enhance the differentiation of human mesenchymal stem cells (MSCs), which also showed robust new bone formation with this Ti-GO-BMP2 implant, as demonstrated by Char et al. [128]; in

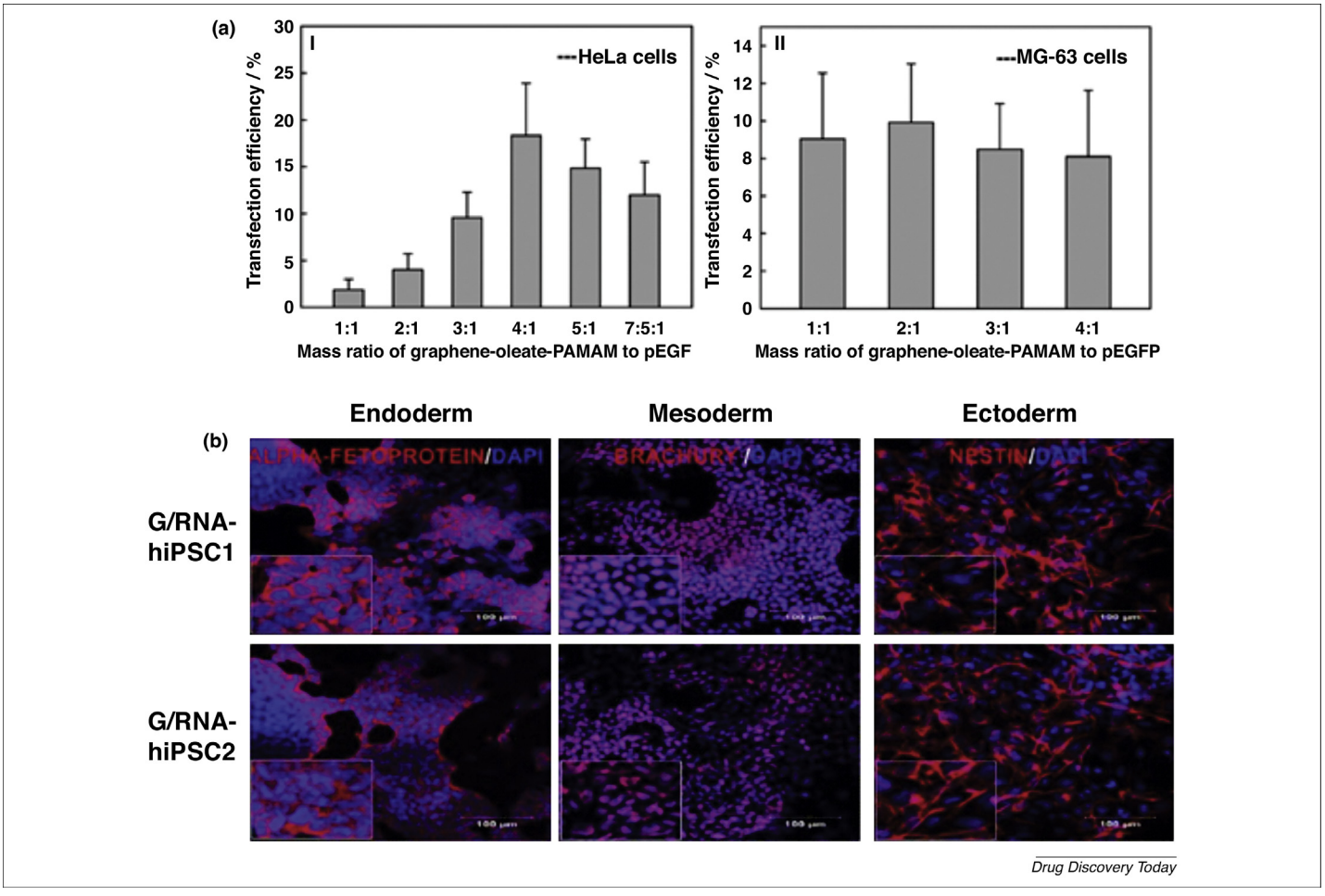

FIGURE 4

Graphene-based nanomaterials for gene delivery . (a) GFP transfection efficiency of graphene-oleate-polyamidoamine (PAMAM) to HeLa (i) and MG-63 (ii) cells. (b) *In vitro* differentiation potentials of GO-PEI-RNA-iPSC clones from hADFs were analyzed according to the expression of protein markers from each of the three germ layers (endoderm: alpha-fetoprotein, mesoderm: brachyury, ectoderm: nestin, all shown in red) using immunocytochemistry. Adapted, with permission, from [121] (a) and [84] (b).

addition, Geest and co-workers reported the intracellular protein vaccine delivery of GO-adsorbed proteins that could be efficiently internalized by dendritic cells and promoted antigen cross-presentation to CD8 T cells [129].

Bioimaging

Bioimaging has a crucial role in both research and clinical practice, and allows the observation and study of biological processes from the subcellular to small-animal level [130,131]. With the appropriate probe, bioimaging enables us to detect early-stage disease and to monitor the treatment response [130]. The versatile surface functionality of graphene-based materials for conjugating small-molecular dyes, fluorescent NPs, or biomolecules, combined with their intrinsic luminescent properties, renders these materials ideal agents for bioimaging applications [131,132]. Here, we mainly focus on the optical imaging of graphene-based nanomaterials in biological applications.

The intrinsic photoluminescence of nGO can be used for fluorescence imaging, as first reported by Dai et al. These authors prepared PEG-GO covalently conjugated with the B cell-specific antibody rituxan (anti-CD20) (nGO–PEG–Rituxan) for Raji B cell-targeted fluorescence imaging in the near-infrared region with little background [101]. However, the low quantum yield of nGO-PEG fluorescence greatly limited the further *in vivo* fluorescent imaging of animals. To overcome this limitation, fluorescent dyes were used to functionalize GO either covalently or noncovalently to enhance the fluorescent signal for *in vitro* and *in vivo* imaging. For example, Liu et al. covalently labeled nGO-PEG with a Cy7 dye (nGO-PEG-Cy7) for *in vivo* fluorescent imaging of tumor-xenografted mice, showing ultrahigh tumor accumulation of nGO-PEG-Cy7 based on the enhanced permeability and retention effect of cancerous tumors [133]. Chen et al. reported VEGF-loaded IR800-conjugated GO (GO-IR800-VEGF) for imaging ischemic muscle tissue in a murine hind limb ischemia model [134]. They demonstrated that the *in vivo* pharmacokinetics and biodistribution of GO-IR800-VEGF could be successfully monitored by NIR fluorescence imaging, indicating the potential of using GO in theranostic applications for treating ischemic disease. In addition to covalent functionalization, the direct loading of dyes or other photosensitizers was also investigated for fluorescence imaging. Chen et al. developed sinoporphyrin sodium (DVDMS)-loaded GO-PEG (GO-PEG-DVDMS) with improved fluorescent properties for enhanced optical imaging [135]. The fluorescent property of DVDMS was significantly enhanced because of the intramolecular charge transfer between DVDMS and GO-PEG, which enabled the use of GO-PEG-DVDMS for real-time fluorescent visualization of *in vivo* DVDMS delivery and distribution.

In addition to GO, GQDs with quantum confinement and edge effects have unique optical properties that can be used for bioimaging applications. GQDs have a wide optical absorption, from UV to near-infrared, with the strongest peak located in the UV region. The fluorescence color depends on the size of GQDs and GQDs with green and blue fluorescence have now been developed [56,112,136]. Zhu et al. used GQDs for conventional bioimaging by incubating human osteosarcoma cells with GQD suspensions [112]. The GQDs translocated into the cell via the cell membrane and were observed successfully, using a confocal fluorescence microscope. Cationic GQDs have a tendency to aggregate in aqueous solution, therefore, GQDs modified with biocompatible polymers are preferred. Dong et al. functionalized GQDs with poly (L-lactide) (PLA) and PEG for intracellular miRNA imaging analysis combined with gene delivery with improved therapeutic efficiency [137]. The PLA-PEG-grafted-GQDs exhibited excellent physiological stability and stable photoluminescence. PLA-PEG-grafted-GQDs conjugated to agents targeting miRNA-21 and survivin, as a gene vector into Hela cells, were observed to fluoresce green inside cells under a confocal microscope, which enabled better observation and regulation of the gene delivery. Wen et al. fabricated fluorescent organosilane-functionalized GQDs (Si-GQDs) that were then embedded into mesoporous hollow silica nanospheres [138]. In the *in vitro* cellular uptake experiments in HePG2 cells, the hybrid nanospheres exhibited blue and green colors under excitation at 405 nm and 488 nm, respectively. The results showed functionalized GQDs to be promising candidates for bioimaging applications to help monitoring drug or gene delivery.

In addition to fluorescence imaging, Yang et al. recently reported a novel label-free highly sensitive imaging method for the fast visualization and quantitative layer analysis of graphene and GO, as well as real-time imaging of GO *in vitro* with cells and *ex vivo* in circulating blood, based on the transient absorption process [139]. They used megahertz modulation that effectively avoided the low-frequency laser noise and a resonant circuit that electronically amplified the heterodyne-detected signal. With this imaging platform, they achieved high-speed imaging of GO in living cells and animals with the capability of quantitative analysis of the intracellular concentration of well-dispersed PEG-GO (Fig. 5), opening new opportunities for using GO as a bioimaging agent based on the transient absorption imaging method.

Raman spectra of graphene-based nanomaterials have also been applied for bioimaging. Both graphene and GO exhibit unique intrinsic Raman signals that can be further enhanced by integrating metal NPs [140–144]. Tan and Zhang et al. reported the facile synthesis of AgCu@graphene (ACG) NPs by growing several layers of graphene onto the surface of AgCu alloy NPs using the chemical vapor deposition method [140]. The ACG NPs have been utilized to enhance unique Raman signals from the graphitic shell, making ACG an ideal candidate for cell labeling, rapid Raman imaging, and surface-enhanced Raman spectroscopy (SERS) detection. *In situ* reduction of metal ions on GO results in stronger Raman signals from metal–GO hybrids compared with the pristine GO. Guo et al. developed GO-Ag NP composites by *in situ* reducing Ag^+ using polyvinylpyrrolidone as a novel SERS label for fast cellular probing and imaging [141]. The authors demonstrated that, by utilizing GO-Ag NPs as a highly sensitive optical probe, fast SERS imaging of cancer cells was realized with a short integration time of approximately 0.06 s per pixel. Zhao and co-workers reported the one-step synthesis of nanosized GO-wrapped gold NPs [142]. These GO-Au nanocomposites could be utilized for both intracellular bioimaging tags and drug delivery carriers. Similar results were also reported by Liz-Marzan and co-workers [143]. Noncovalent attachment of Au NPs to GO via π–π stacking or other molecular interactions has also been used for Raman imaging. Zhang et al. reported that the presence of Au NPs on the GO sheet has an important role in the observation of enhanced Raman spectra of GO in live cells [144]. In addition to these optical imaging methods, graphene-based nanomaterials have also been

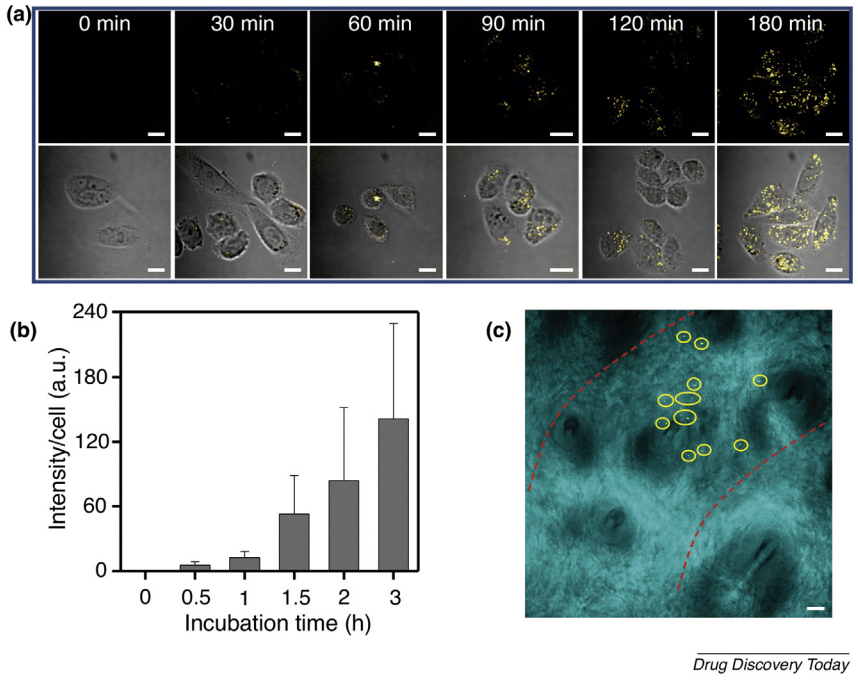

FIGURE 5

Transient absorption imaging of GO. (a) Dynamic cellular uptake of GO-PEG was monitored by TA imaging overtime, from 0 to 180 min after treatment. TA images (first row) and overlay images (second row) showed intracellular accumulation of GO-PEG (yellow dots). Scale bar = 10 mm. (b) Quantification of mean TA signal intensity per cell in GO-PEG treated cells from (a). (c) TA imaging of GO-PEG circulating in rat blood vessel. Scale bar = 20 mm. Adapted, with permission, from [139].

used for other imaging modalities, including photoacoustic imaging [145], magnetic resonance imaging [146], computed tomography [147], as well as radionuclide-based imaging, such as positron emission tomography and single-photon emission computed tomography [148,149]. However, due to the space constraints, we do not discuss them in detail here.

Tissue engineering

Tissue engineering has emerged as a significant novel medical strategy to restore, maintain, or improve the function of a tissue or whole organ by using a combination of cells, engineering materials, and suitable biochemical factors [150]. A crucial parameter for tissue engineering is to develop suitable biomaterials that can mimic the biological environment and provide surfaces to interface with living cells, enabling cell attachment, proliferation, and differentiation. Given their ease of functionalization combined with fascinating mechanical strength, stiffness, and electrical conductivity, graphene-based materials have attracted tremendous interest in the tissue-engineering field [151,152].

One application of graphene-based materials in tissue engineering is as reinforcement materials in hydrogels, films, fibers, and other tissue-engineering scaffolds, to enhance their mechanical properties and stability by utilizing the mechanical strength and stiffness of graphene-based materials. Cerruti et al. prepared a 3D GO/HA hydrogel for bone tissue engineering [153]. The resulting highly porous hydrogel showed strong mechanical properties, high electrical conductivity, and good cell compatibility to MSCs, making them excellent candidates for bone tissue-engineering applications. GO nanosheets have also been shown to greatly improve the mechanical properties of poly(acrylic acid) (PAA)/gelatin hydrogels and chitosan hydrogel scaffolds [154,155]. Additionally, Ruoff and co-workers presented polyoxyethylene sorbitan laurate (TWEEN) and rGO hybrid films [156]. They demonstrated that the as-prepared hybrid films were mechanically robust, biocompatible with three different mammalian cell lines, and antimicrobial. Xie et al. prepared chitosan-poly (vinyl alcohol) nanofiber-containing graphene by using the electrospinning method [157]. They found that these reinforced fibers showed rapid wound healing in mice and rabbits because of the presence of free electrons in graphene inhibiting prokaryotic cell multiplication but without affecting the proliferation of eukaryotic cells.

In addition to mechanical enhancement, the electrical properties of graphene-based materials enable researchers to use them for specific tissue-engineering applications. Hong et al. reported that a graphene substrate promoted the adhesion and neural differentiation of human neural stem cells (hNSCs) [158]. The authors proposed that the mechanism of enhanced differentiation to neurons was electrical coupling between the hNSCs and the graphene. Cheng et al. demonstrated the promotion of neurite sprouting and outgrowth of mouse hippocampal cells on graphene substrates [159]. They speculated that the high electrical conductivity of graphene led to better neurite outgrowth, indicating that graphene could be used as an implant material or neural chip for tissue engineering in the nervous system. Similar results were also reported by Liu et al. [160]. Recently, Wang and co-workers reported a hybrid conducting system of poly(3,4-ethylenedioxythiophene) (PEDOT)-rGO microfibers [161]. These hybrid microfibers exhibited enhanced cell proliferation and improved neural differentiation of MSCs with electrical pulses induced by a self-powered triboelectric nanogenerator. Loh et al. studied the culture

of bone marrow-derived MSCs on graphene and GO substrates [162]. They found that the strong noncovalent binding abilities of graphene arising from π–π stacking, electrostatic, and hydrogen bonding allowed it to act as a preconcentration platform for osteogenic inducers, which accelerated the growth of MSCs toward the osteogenic lineage.

In addition to their mechanical and electrical properties, the surface functionalization of graphene-based materials is also useful for tissue-engineering applications. Gu et al. reported that amine-functionalized GO showed superior cell viability and proliferation with excellent anticoagulation effects [163]. Estrada and co-workers reported the elongated structure of multinucleated myoblasts on laminin-coated graphene, indicating their differentiation into myotube cells [164]. GO has also been shown to help cells differentiate into skeletal muscle, likely because of their roughness and serum protein absorption [165]. It is also believed that absorbing fibronectin on a graphene-based material surface would promote articular cartilage regeneration [166]. GO has been found to help adipose tissue generation, the mechanism of which was attributed to absorption of insulin [162]. Additionally, Zeng et al. reported gelatin-functionalized GO (GO-Gel) for the biomimetic mineralization of HA [167]. They demonstrated that the GO-Gel promoted cell adhesion, proliferation, and osteogenic differentiation of MC3T3-E1 cells, indicating that GO-Gel could be used as osteogenesis-promoting scaffold for bone tissue engineering. Zeng and co-workers also reported similar results using GO functionalized with the polysaccharide carrageenan [168].

In addition, the chemical inertness and impermeability of graphene enable it to be used as a biocompatible anticorrosion coating for metallic biomedical devices. Rao et al. reported that graphene coating enhanced both the bio- and hemocompatibility of implant materials [169,170]. Yang and co-workers demonstrated the use of graphene as a protection film in biological environments [171]. They conducted both *in vitro* cellular experiments and *in vivo* animal experiments to demonstrate the effective protection of metal by graphene under biological conditions (Fig. 6). Their results highlight the potential of using graphene coatings to protect metal surfaces in biomedical applications, such as metal implants. Wei et al. reported that a GO/HA-coated Ti substrate also exhibited high corrosion resistance, with enhanced coating adhesion strength and superior cell viability [172].

Toxicity of graphene-based nanomaterials

So far, graphene-based materials have exhibited huge potential in numerous biomedical applications. To further expand their use and advance the translation of these applications from the lab to a

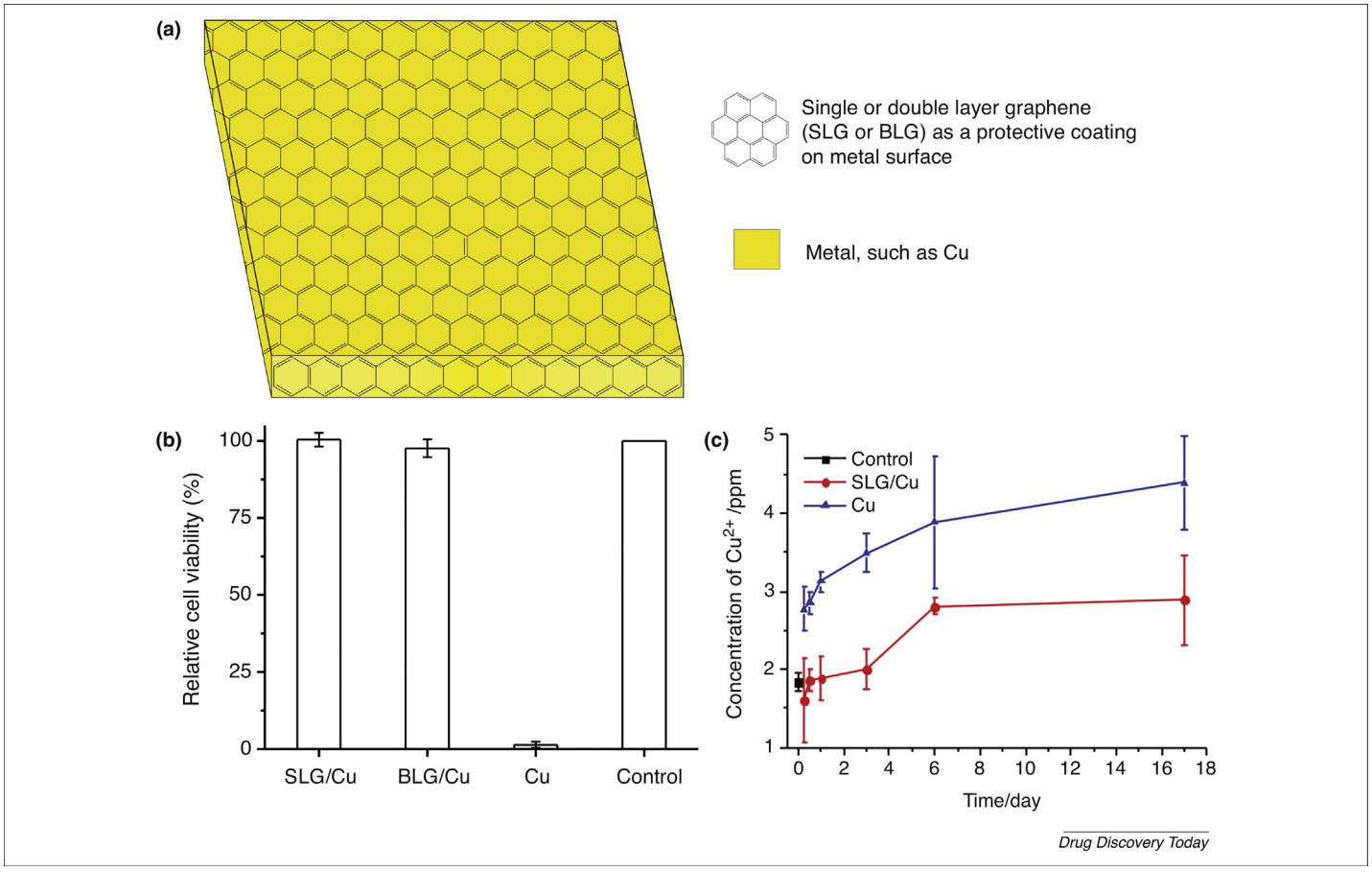

FIGURE 6

Graphene as a protective coating in biological environments. (a) Schematic illustration of graphene as a protective layer on a metal surface. (b) Relative cell viability of bone cells incubated with SLG/Cu, BLG/Cu, and bare Cu foil for 1 day. The control was the regular cell culture without the presence of any form of Cu foil. (c) Concentration of Cu^{2+} ions in blood extracted from live rats. Concentrations of Cu^{2+} ions from normal rats before implantation as control (black square), rats with implanted SLG/Cu foils (blue triangles), and rats with implanted Cu foils (red dots) as a function of time after implantation. Adapted, with permission, from [171].

clinical setting, a deeper understanding of their potential toxicity is required. Intense efforts have been devoted to elucidating the toxic effects of graphene and its derivatives. However, the molecular mechanism of the toxicity of graphene-based materials is still largely unclear. For example, recent studies obtained contradictory outcomes that observed both toxic and nontoxic effects simultaneously when evaluating the *in vitro* and *in vivo* toxicity of graphene [156,173,174]. Therefore, it is currently inappropriate to draw any generalized conclusions about the toxic effects of graphene-based materials, particularly when regarding the variety of different forms of graphene and methods of synthesis. Here, we briefly summarize and discuss the current state-of-the art of toxicity studies of graphene-based materials.

Graphene and its related congeners have been reported to cause cell damage via inducing generations of reactive oxidant species [160,175] and/or mutations during cell replication [176,177]. Their toxicity has been demonstrated to be time [178,179], dose and/or concentration [178,180], and characteristic [177] dependent. Cell–graphene interactions *in vitro* have been shown to depend on multiple parameters, including surface chemistry, graphene size and/or shape, and impurities.

The surface chemistry of graphene has an essential role in determining its cytotoxicity. Generally, bare graphene or GO can interfere with the cell membrane via adhesion or bonding with cell receptors to block the supply of nutrients, induce stress, and activate apoptotic mechanisms, resulting in high toxicity even at low concentrations [181]. Functionalization of graphene-based materials with biocompatible polymers or molecules will greatly reduce cytotoxicity. Dai et al. showed that PEGylation of GO exhibited no cellular toxicity up to 100 mg/ml [18,101]. Alexis and co-workers reported that graphene with PEG and PLA modification showed no dose-dependent toxicity up to 250 mg/ml for U138 cells, whereas hydroxylated graphene showed toxicity at 50 mg/ml in the same study [182]. Curley et al. found that sulfonated GO was nontoxic across the concentration range of 0.1–10 mg/ml [183]. Additionally, carboxylation [184], dextran conjugation [185,186], and PEI [123] have also been demonstrated to reduce graphene cytotoxicity, by increasing the hydrophilicity of graphene derivatives.

In addition to surface functionalization, the size of graphene nanomaterials also affects their interaction with cells and their cytotoxicity. Wang et al. studied the *in vitro* toxicity of GO on A549 cells [180]. They reported that graphene oxide of size 160 ± 90 nm induced less cell mortality compared with 780 ± 410 nm at the same concentration of 200 mg/ml. However, larger size does not always cause less cytotoxicity. Akhavan and collaborators indicated that, in human MSC, rGO nanoplatelets with smaller lateral dimensions (11 ± 4 nm) showed higher cytotoxicity than those with larger lateral dimensions (3.8 ± 0.4 mm) [177]. These contradictory observations could be explained by different interactions between cells and particles with different sizes, because Yan et al. demonstrated that small nanosheets entered cells mainly via clathrin-mediated endocytosis, while the increase in graphene size enhanced the phagocytotic uptake of the nanosheets [187].

Impurities from the preparation process of GO could affect its biocompatibility. Kostarelos and co-workers reported that purified GO had negligible negative effects *in vitro* and *in vivo* compared with as-synthesized GO [188]. Therefore, it is necessary to conduct careful biological effects studies of these impurities.

In addition to *in vitro* studies, experiments were also performed *in vivo* to investigate graphene toxicity, which demonstrates more complexity when animal models are used. Typically, after intravenous injection, graphene materials were found in spleen, liver, and lung. However, Liu et al. reported that intraperitoneal injection of PEGylated graphene resulted in accumulation in spleen and liver, instead of lung [189]. By contrast, when graphene materials are administered via inhalation, they typically accumulate in the lung and often induce inflammation [190]. Intraocular administration of GO was studied in rabbits, and showed little effect on eyeball appearance, intraocular pressure eyesight, or histology sections [191]. Dash and collaborators reported that intravenous administration of GO induced extensive pulmonary thromboembolism in mice [192], whereas fewer effects were observed for rGO in the same study. Contradictory results were also observed in *in vivo* experiments, because GO was found to induce high hemolytic activity [193], which was inconsistent with the results of Wang et al. who reported that intravenous injection of GO at 0.1 mg and 0.25 mg showed no obvious toxicity [194]. Thus, we are still some way from completely understanding the toxicity of graphene-based materials.

Concluding remarks

Here, we have reviewed the biomedical applications of graphene-based nanomaterials, including drug and/or gene delivery, bioimaging, and tissue engineering. Different types of graphene, its derivatives and composites have been introduced, and their properties related to biomedical applications have been discussed. The outstanding properties, such as a large specific surface area, excellent mechanical strength, and unique optical properties, of graphene-based materials, make them ideal candidates to load various drugs or genes for delivery, to act as imaging agents, as well as to enhance the mechanical properties of biomaterials for tissue engineering. Examples of these versatile applications have been presented here. Finally, we have also discussed the potential toxicity of these materials, even though the detailed toxic mechanisms remain uncertain or contradictory. Overall, we believe that graphene-based materials will open a new biomedical era. However, more efforts are required to completely elucidate the toxic principle of these materials before they can progress to clinical trials.

References

1 Novoselov, K.S. *et al.* (2004) Electric field effect in atomically thin carbon films. *Science* 306, 666–669

2 Novoselov, K.S. *et al.* (2005) Two-dimensional atomic crystals. *Proc. Natl. Acad. Sci. U. S. A.* 102, 10451–10453

3 Geim, A.K. (2009) Graphene: status and prospects. *Science* 324, 1530–1534

4 Geim, A.K. and Novoselov, K.S. (2007) The rise of graphene. *Nat. Mater.* 6, 183–191

5 Kuila, T. *et al.* (2013) Recent advances in the efficient reduction of graphene oxide and its application as energy storage electrode materials. *Nanoscale* 5, 52–71

6 Tozzini, V. and Pellegrini, V. (2013) Prospects for hydrogen storage in graphene. *Phys. Chem. Chem. Phys.* 15, 80–89

7 Pumera, M. (2011) Graphene in biosensing. *Mater. Today* 14, 308–315
8 Kuila, T. *et al.* (2011) Recent advances in graphene-based biosensors. *Biosens. Bioelectron.* 26, 4637–4648
9 Zhang, K. *et al.* (2010) Graphene-polyaniline nanofiber composites as supercapacitor electrodes. *Chem. Mater.* 22, 1392–1401
10 Rao, C.N. *et al.* (2009) Graphene: the new two-dimensional nanomaterial. *Angew. Chem. Int. Ed.* 48, 7752–7777
11 Balandin, A.A. *et al.* (2008) Superior thermal conductivity of single-layer graphene. *Nano Lett.* 8, 902–907
12 Latil, S. and Henrard, L. (2006) Charge carriers in few-layer graphene films. *Phys. Rev. Lett.* 97, 036803
13 Chen, D. *et al.* (2010) Graphene-based materials in electrochemistry. *Chem. Soc. Rev.* 39, 3157–3180
14 Stoller, M.D. *et al.* (2008) Graphene-based ultracapacitors. *Nano Lett.* 8, 3498–3502
15 Lee, C. *et al.* (2008) Measurement of the elastic properties and intrinsic strength of monolayer graphene. *Science* 321, 385–388
16 Bolotin, K.I. *et al.* (2008) Ultrahigh electron mobility in suspended graphene. *Solid State Commun.* 146, 351–355
17 Morozov, S.V. *et al.* (2008) Giant intrinsic carrier mobilities in graphene and its bilayer. *Phys. Rev. Lett.* 100, 016602
18 Liu, Z. *et al.* (2008) PEGylated nanographene oxide for delivery of water-insoluble cancer drugs. *J. Am. Chem. Soc.* 130, 10876–10877
19 Yang, W.R. *et al.* (2010) Carbon nanomaterials in biosensors: should you use nanotubes or graphene? *Angew. Chem. Int. Ed.* 49, 2114–2138
20 Allen, M.J. *et al.* (2010) Honeycomb carbon: a review of graphene. *Chem. Rev.* 110, 132–145
21 Compton, O.C. and Nguyen, S.T. (2010) Graphene oxide, highly reduced graphene oxide, and graphene: versatile building blocks for carbon-based materials. *Small* 6, 711–723
22 Yoo, J.M. (2015) Graphene-based nanomaterials for versatile imaging studies. *Chem. Soc. Rev.* 44, 4835–4852
23 Goenka, S. *et al.* (2014) Graphene-based nanomaterials for drug delivery and tissue engineering. *J. Control. Release* 173, 75–88
24 Hummers, W.S. and Offeman, R.E. (1958) Preparation of graphitic oxide. *J. Am. Chem. Soc.* 80 1339–1339
25 Cote, L.J. *et al.* (2009) Langmuir-blodgett assembly of graphite oxide single layers. *J. Am. Chem. Soc.* 131, 1043–1049
26 Chen, D. *et al.* (2012) Graphene oxide: preparation, functionalization, and electrochemical applications. *Chem. Rev.* 112, 6027–6053
27 Eda, G. and Chhowalla, M. (2010) Chemically derived graphene oxide: towards large-area thin-film electronics and optoelectronics. *Adv. Mater.* 22, 2392–2415
28 Li, X. *et al.* (2008) Highly conducting graphene sheets and Langmuir-Blodgett films. *Nat. Nanotechnol.* 3, 538–542
29 Lerf, A. *et al.* (1998) Structure of graphite oxide revisited. *J. Phys. Chem. B* 102, 4477–4482
30 Paredes, J.I. *et al.* (2008) Graphene oxide dispersions in organic solvents. *Langmuir* 24, 10560–10564
31 Nurunnabi, M. *et al.* (2015) Bioapplication of graphene oxide derivatives: drug/gene delivery, imaging, polymeric modification, toxicology, therapeutics and challenges. *RSC Adv.* 5, 42141–42161
32 Xu, C. *et al.* (2015) Fabrication and characteristics of reduced graphene oxide produced with different green reductants. *PLoS One* 10, e0144842
33 Tung, V.C. *et al.* (2009) High-throughput solution processing of large-scale graphene. *Nat. Nanotechnol.* 4, 25–29
34 Chua, C.K. and Pumera, M. (2016) The reduction of graphene oxide with hydrazine: elucidating its reductive capability based on a reaction-model approach. *Chem. Commun.* 52, 72–75
35 Abdolhosseinzadeh, S. *et al.* (2015) Fast and fully-scalable synthesis of reduced graphene oxide. *Sci. Rep.* 5, 10160
36 Zhang, J. *et al.* (2010) Reduction of graphene oxide vial-ascorbic acid. *Chem. Commun.* 46, 1112–1114
37 Shin, H.-J. *et al.* (2009) Efficient reduction of graphite oxide by sodium borohydride and its effect on electrical conductance. *Adv. Funct. Mater.* 19, 1987–1992
38 Chua, C.K. and Pumera, M. (2013) Reduction of graphene oxide with substituted borohydrides. *J. Mater. Chem. A* 1, 1892–1898
39 Wang, G. *et al.* (2008) Facile synthesis and characterization of graphene nanosheets. *J. Phys. Chem. C* 112, 8192–8195
40 Bourlinos, A.B. *et al.* (2003) Graphite oxide: chemical reduction to graphite and surface modification with primary aliphatic amines and amino acids. *Langmuir* 19, 6050–6055
41 Song, P. *et al.* (2012) Synthesis of graphene nanosheetsviaoxalic acid-induced chemical reduction of exfoliated graphite oxide. *RSC Adv.* 2, 1168–1173
42 Fernández-Merino, M.J. *et al.* (2010) Vitamin C is an ideal substitute for hydrazine in the reduction of graphene oxide suspensions. *J. Phys. Chem. C* 114, 6426–6432
43 Dreyer, D.R. *et al.* (2011) Reduction of graphite oxide using alcohols. *J. Mater. Chem.* 21, 3443–3447
44 Bo, Z. *et al.* (2014) Green preparation of reduced graphene oxide for sensing and energy storage applications. *Sci. Rep.* 4, 4684
45 Lin, X. *et al.* (2012) Fabrication of highly-aligned, conductive, and strong graphene papers using ultralarge graphene oxide sheets. *ACS Nano* 6, 10708–10719
46 Zhao, J. *et al.* (2010) Efficient preparation of large-area graphene oxide sheets for transparent conductive films. *ACS Nano* 4, 5245–5252
47 Bai, H. *et al.* (2009) Non-covalent functionalization of graphene sheets by sulfonated polyaniline. *Chem. Commun.* 1667–1669
48 Zu, S.-Z. and Han, B.-H. (2009) Aqueous dispersion of graphene sheets stabilized by pluronic copolymers: formation of supramolecular hydrogel. *J. Phys. Chem. C* 113, 13651–13657
49 Hao, R. *et al.* (2008) Aqueous dispersions of TCNQ-anion-stabilized graphene sheets. *Chem. Commun.* 6576–6578
50 Xu, Y. *et al.* (2008) Flexible graphene films via the filtration of water-soluble noncovalent functionalized graphene sheets. *J. Am. Chem. Soc.* 130, 5856–5857
51 Jin, L. *et al.* (2016) Fabrication, characterization, and biocompatibility of polymer cored reduced graphene oxide nanofibers. *ACS Appl. Mater Interfaces* 8, 5170–5177
52 Cardenas, L. *et al.* (2014) Reduced graphene oxide growth on 316L stainless steel for medical applications. *Nanoscale* 6, 8664–8670
53 Zhang, X.-F. and Gurunathan, S. (2016) Biofabrication of a novel biomolecule-assisted reduced graphene oxide: an excellent biocompatible nanomaterial. *Int. J. Nanomed.* 11, 15
54 Tang, L. *et al.* (2012) Deep ultraviolet photoluminescence of water-soluble self-passivated graphene quantum dots. *ACS Nano* 6, 5102–5110
55 Liu, R. *et al.* (2011) Bottom-up fabrication of photoluminescent graphene quantum dots with uniform morphology. *J. Am. Chem. Soc.* 133, 15221–15223
56 Pan, D. *et al.* (2010) Hydrothermal route for cutting graphene sheets into blue-luminescent graphene quantum dots. *Adv. Mater.* 22, 734–738
57 Qu, D. *et al.* (2014) Formation mechanism and optimization of highly luminescent N-doped graphene quantum dots. *Sci. Rep.* 4, 5294
58 Peng, J. *et al.* (2012) Graphene quantum dots derived from carbon fibers. *Nano Lett.* 12, 844–849
59 Favaro, M. *et al.* (2015) Single and multiple doping in graphene quantum dots: unraveling the origin of selectivity in the oxygen reduction reaction. *ACS Catal.* 5, 129–144
60 Schnez, S. *et al.* (2009) Observation of excited states in a graphene quantum dot. *Appl. Phys. Lett.* 94, 012107
61 Yan, X. *et al.* (2010) Synthesis of large, stable colloidal graphene quantum dots with tunable size. *J. Am. Chem. Soc.* 132, 5944–5945
62 Lu, J. *et al.* (2011) Transforming C60 molecules into graphene quantum dots. *Nat. Nanotechnol.* 6, 247–252
63 Wang, L. *et al.* (2014) Gram-scale synthesis of single-crystalline graphene quantum dots with superior optical properties. *Nat. Commun.* 5, 5357
64 Guo, C.X. *et al.* (2010) Layered graphene/quantum dots for photovoltaic devices. *Angew. Chem. Int. Ed.* 49, 3014–3017
65 Girit, Ç.Ö. *et al.* (2009) Graphene at the edge: stability and dynamics. *Science* 323, 1705–1708
66 Gupta, V. *et al.* (2011) Luminescent graphene quantum dots for organic photovoltaic devices. *J. Am. Chem. Soc.* 133, 9960–9963
67 Shtein, M. *et al.* (2015) Characterization of graphene-nanoplatelets structure via thermogravimetry. *Anal. Chem.* 87, 4076–4080
68 Li, L. *et al.* (2013) Focusing on luminescent graphene quantum dots: current status and future perspectives. *Nanoscale* 5, 4015–4039
69 Buzaglo, M. *et al.* (2016) Graphene quantum dots produced by microfluidization. *Chem. Mater.* 28, 21–24
70 Yang, S.-T. *et al.* (2009) Carbon dots for optical imaging *in vivo*. *J. Am. Chem. Soc.* 131, 11308–11309
71 Baker, S.N. and Baker, G.A. (2010) Luminescent carbon nanodots: emergent nanolights. *Angew. Chem. Int. Ed.* 49, 6726–6744
72 Ran, X. *et al.* (2013) Ag nanoparticle-decorated graphene quantum dots for label-free, rapid and sensitive detection of Ag+ and biothiols. *Chem. Commun.* 49, 1079–1081
73 Sun, H. *et al.* (2015) Synthesis of fluorinated and nonfluorinated graphene quantum dots through a new top-down strategy for long-time cellular imaging. *Chem. Eur. J.* 21, 3791–3797
74 Ge, J. *et al.* (2015) Red-emissive carbon dots for fluorescent, photoacoustic, and thermal theranostics in living Mice. *Adv. Mater.* 27, 4169–4177
75 Ge, J. *et al.* (2014) A graphene quantum dot photodynamic therapy agent with high singlet oxygen generation. *Nat. Commun.* 5, 4596

76 Zhang, Q. *et al.* (2014) Synthesis of amphiphilic reduced graphene oxide with an enhanced charge injection capacity for electrical stimulation of neural cells. *J. Mater. Chem. B* 2, 4331–4337
77 Chen, W. *et al.* (2015) Assembly of Fe3O4 nanoparticles on PEG-functionalized graphene oxide for efficient magnetic imaging and drug delivery. *RSC Adv.* 5, 69307–69311
78 Shi, S. *et al.* (2014) Surface engineering of graphene-based nanomaterials for biomedical applications. *Bioconjugate Chem.* 25, 1609–1619
79 Zhang, C. *et al.* (2016) Co-delivery of paclitaxel and indocyanine green by PEGylated graphene oxide: a potential integrated nanoplatform for tumor theranostics. *RSC Adv.* 6, 15460–15468
80 Jin, R. *et al.* (2013) Self-assembled graphene-dextran nanohybrid for killing drug-resistant cancer cells. *ACS Appl. Mater Interfaces* 5, 7181–7189
81 Lee, Y. *et al.* (2015) Injectable and mechanically robust 4-arm PPO-PEO/graphene oxide composite hydrogels for biomedical applications. *Chem. Commun.* 51, 8876–8879
82 Deshmukh, K. *et al.* (2016) Graphene oxide reinforced polyvinyl alcohol/polyethylene glycol blend composites as high-performance dielectric material. *J. Polym. Res.* 23, 159
83 Teimouri, M. *et al.* (2016) Graphene oxide-cationic polymer conjugates synthesis and application as gene delivery vectors. *Plasmid* 84–85, 51–60
84 Choi, H.Y. *et al.* (2016) Efficient mRNA delivery with graphene oxide-polyethylenimine for generation of footprint-free human induced pluripotent stem cells. *J. Control. Release* 235, 222–235
85 Cao, X. *et al.* (2015) Functionalized graphene oxide with hepatocyte targeting as anti-tumor drug and gene intracellular transporters. *J. Nanosci. Nanotechnol.* 15, 2052–2059
86 Hu, H. *et al.* (2014) Folate conjugated trimethyl chitosan graphene oxide nanocomplexes as potential carriers for drug and gene delivery. *Mater. Lett.* 125, 82–85
87 Wu, S. *et al.* (2015) High concentration and stable aqueous dispersion of graphene stabilized by a new amphiphilic copolymer Fullerene, Nanotubes. *Carbon Nanostruct.* 23, 974–984
88 Solanki, A. *et al.* (2013) Axonal alignment and enhanced neuronal differentiation of neural stem cells on graphene-nanoparticle hybrid structures. *Adv. Mater.* 25, 5477–5482
89 Zhou, X. *et al.* (2014) A quantitative study of the intracellular concentration of graphenenoble metal nanocomposites and their cytotoxicity. *Nanoscale* 6, 8535–8542
90 Chen, H. *et al.* (2015) Fe2O3@Au core@shell nanoparticle-graphene nanocomposites as theranostic agents for bioimaging and chemo-photothermal synergistic therapy. *RSC Adv.* 5, 84980–84987
91 Peng, E. *et al.* (2012) Synthesis of manganese ferrite/graphene oxide nanocomposites for biomedical applications. *Small* 8, 3620–3630
92 Dinda, S. *et al.* (2016) Grafting of ZnS:Mn-doped nanocrystals and an anticancer drug onto graphene oxide for delivery and cell labeling. *ChemPlusChem* 81, 100–107
93 Lee, J.H. *et al.* (2015) Reduced graphene oxide-coated hydroxyapatite composites stimulate spontaneous osteogenic differentiation of human mesenchymal stem cells. *Nanoscale* 7, 11642–11651
94 Lee, W.C. *et al.* (2015) Cell-assembled graphene biocomposite for enhanced chondrogenic differentiation. *Small* 11, 963–969
95 Gao, W. *et al.* (2009) New insights into the structure and reduction of graphite oxide. *Nat. Chem.* 1, 403–408
96 Zhu, Y. *et al.* (2010) Graphene and graphene oxide: synthesis, properties, and applications. *Adv. Mater.* 22, 3906–3924
97 Soldano, C. *et al.* (2010) Production, properties and potential of graphene. *Carbon* 48, 2127–2150
98 Loh, K.P. *et al.* (2010) The chemistry of graphene. *J. Mater. Chem.* 20, 2277–2289
99 Viswanathan, S. *et al.* (2015) Graphene-protein field effect biosensors: glucose sensing. *Mater. Today* 18, 513–522
100 Georgakilas, V. *et al.* (2016) Noncovalent functionalization of graphene and graphene oxide for energy materials, biosensing, catalytic, and biomedical applications. *Chem. Rev.* 116, 5464–5519
101 Sun, X. *et al.* (2008) Nano-graphene oxide for cellular imaging and drug delivery. *Nano Res.* 1, 203–212
102 Zhang, L. *et al.* (2011) Enhanced chemotherapy efficacy by sequential delivery of siRNA and anticancer drugs using PEI-grafted graphene oxide. *Small* 7, 460–464
103 Zhang, L. *et al.* (2010) Functional graphene oxide as a nanocarrier for controlled loading and targeted delivery of mixed anticancer drugs. *Small* 6, 537–544
104 Wang, H. *et al.* (2015) Enhanced mechanical properties of multi-layer graphene filled poly(vinyl chloride) composite films. *J. Mater. Sci. Technol.* 31, 340–344
105 Das, B. *et al.* (2009) Nano-indentation studies on polymer matrix composites reinforced by few-layer graphene. *Nanotechnology* 20 125705
106 Cohen-Karni, T. *et al.* (2010) Graphene and nanowire transistors for cellular interfaces and electrical recording. *Nano Lett.* 10, 1098–1102
107 He, Q. *et al.* (2010) Centimeter-long and large-scale micropatterns of reduced graphene oxide films: fabrication and sensing applications. *ACS Nano* 4, 3201–3208
108 Li, N. *et al.* (2013) Three-dimensional graphene foam as a biocompatible and conductive scaffold for neural stem cells. *Sci. Rep.* 3, 1604
109 Stankovich, S. *et al.* (2006) Stable aqueous dispersions of graphitic nanoplatelets via the reduction of exfoliated graphite oxide in the presence of poly(sodium 4-styrenesulfonate). *J. Mater. Chem.* 16, 155–158
110 Nair, R.R. *et al.* (2008) Fine structure constant defines visual transparency of graphene. *Science* 320 1308–1308
111 Kravets, V.G. *et al.* (2010) Spectroscopic ellipsometry of graphene and an exciton-shifted van Hove peak in absorption. *Phys. Rev. B* 81 155413
112 Zhu, S. *et al.* (2011) Strongly green-photoluminescent graphene quantum dots for bioimaging applications. *Chem. Commun.* 47, 6858–6860
113 Sun, X. *et al.* (2016) A graphene oxide-based FRET sensor for rapid and specific detection of unfolded collagen fragments. *Biosens. Bioelectron.* 79, 15–21
114 Zhang, M. *et al.* (2011) Interaction of peptides with graphene oxide and its application for real-time monitoring of protease activity. *Chem. Commun.* 47, 2399–2401
115 Wang, H. *et al.* (2011) Graphene oxide-peptide conjugate as an intracellular protease sensor for caspase-3 activation imaging in live cells. *Angew. Chem. Int. Ed.* 50, 7065–7069
116 Li, M. *et al.* (2012) Using graphene oxide high near-infrared absorbance for photothermal treatment of Alzheimer's disease. *Adv. Mater.* 24, 1722–1728
117 Zhou, K. *et al.* (2010) One-pot preparation of graphene/Fe3O4 composites by a solvothermal reaction. *New J. Chem.* 34, 2950
118 Xu, Z. *et al.* (2014) Covalent functionalization of graphene oxide with biocompatible poly(ethylene glycol) for delivery of paclitaxel. *ACS Appl. Mater Interfaces* 6, 17268–17276
119 Angelopoulou, A. *et al.* (2015) Graphene oxide stabilized by PLA-PEG copolymers for the controlled delivery of paclitaxel. *Eur. J. Pharm. Biopharm.* 93, 18–26
120 Yang, Z.R. *et al.* (2007) Recent developments in the use of adenoviruses and immunotoxins in cancer gene therapy. *Cancer Gene Ther.* 14, 599–615
121 Liu, X. *et al.* (2014) Polyamidoamine dendrimer and oleic acid-functionalized graphene as biocompatible and efficient gene delivery vectors. *ACS Appl. Mater Interfaces* 6, 8173–8183
122 Tian, B. *et al.* (2011) Photothermally enhanced photodynamic therapy delivered by nano-graphene oxide. *ACS Nano* 5, 7000–7009
123 Feng, L. *et al.* (2011) Graphene based gene transfection. *Nanoscale* 3, 1252–1257
124 Yang, H.-W. *et al.* (2014) Gadolinium-functionalized nanographene oxide for combined drug and microRNA delivery and magnetic resonance imaging. *Nano Res.* 12274
125 Sun, Y. *et al.* (2016) Fabrication of mPEGylated graphene oxide/poly(2-dimethylaminoethyl methacrylate) nanohybrids and their primary application for small interfering RNA delivery. *J. Appl. Polym. Sci.* 133, 43303
126 Shen, H. *et al.* (2012) PEGylated graphene oxide-mediated protein delivery for cell function regulation. *ACS Appl. Mater Interfaces* 4, 6317–6323
127 Choi, M. *et al.* (2015) Multilayered graphene nano-film for controlled protein delivery by desired electro-stimuli. *Sci. Rep.* 5, 17631
128 La, W.-G. *et al.* (2013) Delivery of a therapeutic protein for bone regeneration from a substrate coated with graphene oxide. *Small* 9, 4051–4060
129 Li, H. *et al.* (2016) Spontaneous protein adsorption on graphene oxide nanosheets allowing efficient intracellular vaccine protein delivery. *ACS Appl. Mater Interfaces* 8, 1147–1155
130 Janib, S.M. *et al.* (2010) Imaging and drug delivery using theranostic nanoparticles. *Adv. Drug Delivery Rev.* 62, 1052–1063
131 Lin, J. *et al.* (2016) Graphene-based nanomaterials for bioimaging. *Adv. Drug Delivery Rev.* 105, 242–254
132 Yang, K. *et al.* (2013) Nano-graphene in biomedicine: theranostic applications. *Chem. Soc. Rev.* 42, 530–547
133 Yang, K. *et al.* (2010) Graphene in mice: ultrahigh *in vivo* tumor uptake and efficient photothermal therapy. *Nano Lett.* 10, 3318–3323
134 Sun, Z. *et al.* (2013) VEGF-loaded graphene oxide as theranostics for multi-modality imaging-monitored targeting therapeutic angiogenesis of ischemic muscle. *Nanoscale* 5, 6857–6866
135 Yan, X. *et al.* (2015) Enhanced fluorescence imaging guided photodynamic therapy of sinoporphyrin sodium loaded graphene oxide. *Biomaterials* 42, 94–102

136 Shen, J. *et al.* (2011) Facile preparation and upconversion luminescence of graphene quantum dots. *Chem. Commun.* 47, 2580–2582
137 Dong, H. *et al.* (2015) Multifunctional poly(L-lactide)-polyethylene glycol-grafted graphene quantum dots for intracellular microRNA imaging and combined specific-gene-targeting agents delivery for improved therapeutics. *ACS Appl. Mater Interfaces* 7, 11015–11023
138 Wen, T. *et al.* (2014) Organosilane-functionalized graphene quantum dots and their encapsulation into bi-layer hollow silica spheres for bioimaging applications. *Phys. Chem. Chem. Phys.* 16, 23188–23195
139 Li, J. *et al.* (2015) Highly sensitive transient absorption imaging of graphene and graphene oxide in living cells and circulating blood. *Sci. Rep.* 5, 12394
140 Song, Z.-L. *et al.* (2014) Alkyne-functionalized superstable graphitic silver nanoparticles for Raman imaging. *J. Am. Chem. Soc.* 136, 13558–13561
141 Liu, Z. *et al.* (2013) Graphene oxide based surface-enhanced Raman scattering probes for cancer cell imaging. *Phys. Chem. Chem. Phys.* 15, 2961–2966
142 Ma, X. *et al.* (2013) Graphene oxide wrapped gold nanoparticles for intracellular Raman imaging and drug delivery. *J. Mater. Chem. B* 1, 6495–6500
143 Wang, Y. *et al.* (2014) Reduced graphene oxide-supported gold nanostars for improved SERS sensing and drug delivery. *ACS Appl. Mater Interfaces* 6, 21798–21805
144 Huang, J. *et al.* (2012) Mechanism of cellular uptake of graphene oxide studied by surface-enhanced Raman spectroscopy. *Small* 8, 2577–2584
145 Nie, L. and Chen, X. (2014) Structural and functional photoacoustic molecular tomography aided by emerging contrast agents. *Chem. Soc. Rev.* 43, 7132–7170
146 Kanakia, S. *et al.* (2015) Towards an advanced graphene-based magnetic resonance imaging contrast agent: sub-acute toxicity and efficacy studies in small animals. *Sci. Rep.* 5, 17182
147 Sun, B. *et al.* (2017) In situ synthesis of graphene oxide/gold nanorods theranostic hybrids for efficient tumor computed tomography imaging and photothermal therapy. *Nano Res.* 10, 37–48
148 Shi, S. *et al.* (2017) Chelator-free radiolabeling of nanographene: breaking the stereotype of chelation. *Angew. Chem. Int. Ed.* 56, 2889–2892
149 Fazaeli, Y. *et al.* (2014) *In vivo* SPECT imaging of tumors by 198,199Au-labeled graphene oxide nanostructures. *Mater. Sci. Eng. C* 45, 196–204
150 Langer, R. and Vacanti, J. (1993) Tissue engineering. *Science* 260, 920–926
151 Shin, S.R. *et al.* (2013) Cell-laden microengineered and mechanically tunable hybrid hydrogels of gelatin and graphene oxide. *Adv. Mater.* 25, 6385–6391
152 Cha, C. *et al.* (2014) Controlling mechanical properties of cell-laden hydrogels by covalent incorporation of graphene oxide. *Small* 10, 514–523
153 Xie, X. *et al.* (2015) Graphene and hydroxyapatite self-assemble into homogeneous, free standing nanocomposite hydrogels for bone tissue engineering. *Nanoscale* 7, 7992–8002
154 Faghihi, S. *et al.* (2014) Graphene oxide/poly(acrylic acid)/gelatin nanocomposite hydrogel: experimental and numerical validation of hyperelastic model. *Mater. Sci. Eng. C* 38, 299–305
155 Depan, D. *et al.* (2011) Structure-process-property relationship of the polar graphene oxide-mediated cellular response and stimulated growth of osteoblasts on hybrid chitosan network structure nanocomposite scaffolds. *Acta Biomater.* 7, 3432–3445
156 Park, S. *et al.* (2010) Biocompatible, robust free-standing paper composed of a TWEEN/graphene composite. *Adv. Mater.* 22, 1736–1740
157 Lu, B. *et al.* (2012) Graphene-based composite materials beneficial to wound healing. *Nanoscale* 4, 2978–2982
158 Park, S.Y. *et al.* (2011) Enhanced differentiation of human neural stem cells into neurons on graphene. *Adv. Mater.* 23 (36), H263–H267
159 Li, N. *et al.* (2011) The promotion of neurite sprouting and outgrowth of mouse hippocampal cells in culture by graphene substrates. *Biomaterials* 32, 9374–9382
160 Yang, K. *et al.* (2013) Behavior and toxicity of graphene and its functionalized derivatives in biological systems. *Small* 9, 1492–1503
161 Guo, W. *et al.* (2016) Self-powered electrical stimulation for enhancing neural differentiation of mesenchymal stem cells on graphene-poly(3,4-ethylenedioxythiophene) hybrid microfibers. *ACS Nano* 10, 5086–5095
162 Lee, W.C. *et al.* (2011) Origin of enhanced stem cell growth and differentiation on graphene and graphene oxide. *ACS Nano* 5, 7334–7341
163 Guo, M. *et al.* (2013) N-containing functional groups induced superior cytocompatible and hemocompatible graphene by NH2 ion implantation. *J. Mater. Sci. Mater. Med.* 24, 2741–2748
164 Krueger, E. *et al.* (2016) Graphene foam as a three-dimensional platform for myotube growth. *ACS Biomater. Sci. Eng.* 2, 1234–1241
165 Ku, S.H. and Park, C.B. (2013) Myoblast differentiation on graphene oxide. *Biomaterials* 34, 2017–2023
166 Yoon, H.H. *et al.* (2014) Dual roles of graphene oxide in chondrogenic differentiation of adult stem cells: cell-adhesion substrate and growth factor-delivery carrier. *Adv. Funct. Mater.* 24, 6455–6464
167 Liu, H. *et al.* (2014) Gelatin functionalized graphene oxide for mineralization of hydroxyapatite: biomimetic and in vitro evaluation. *Nanoscale* 6, 5315–5322
168 Liu, H. *et al.* (2014) Biomimetic and cell-mediated mineralization of hydroxyapatite by carrageenan functionalized graphene oxide. *ACS Appl. Mater Interfaces* 6, 3132–3140
169 Podila, R. *et al.* (2013) Graphene coatings for enhanced hemo-compatibility of nitinol stents. *RSC Adv.* 3, 1660–1665
170 Podila, R. *et al.* (2013) Graphene coatings for biomedical implants. *J. Vis. Exp.* 73, e50276
171 Zhang, W. *et al.* (2014) Use of graphene as protection film in biological environments. *Sci. Rep.* 4, 4097
172 Li, M. *et al.* (2014) Graphene oxide/hydroxyapatite composite coatings fabricated by electrophoretic nanotechnology for biological applications. *Carbon* 67, 185–197
173 Bianco, A. (2013) Graphene: safe or toxic? The two faces of the medal. *Angew. Chem. Int. Ed.* 52, 4986–4997
174 Hu, W. *et al.* (2010) Graphene-based antibacterial paper. *ACS Nano* 4, 4317–4323
175 Zhang, Y. *et al.* (2010) Cytotoxicity effects of graphene and single-wall carbon nanotubes in neural phaeochromocytoma-derived PC12 cells. *ACS Nano* 4, 3181–3186
176 Akhavan, O. *et al.* (2013) Genotoxicity of graphene nanoribbons in human mesenchymal stem cells. *Carbon* 54, 419–431
177 Akhavan, O. *et al.* (2012) Size-dependent genotoxicity of graphene nanoplatelets in human stem cells. *Biomaterials* 33, 8017–8025
178 Vallabani, N.V.S. *et al.* (2011) Toxicity of graphene in normal human lung cells (BEAS-2B). *J. Biomed. Nanotechnol.* 7, 106–107
179 Liu, S. *et al.* (2012) Lateral dimension-dependent antibacterial activity of graphene oxide sheets. *Langmuir* 28, 12364–12372
180 Chang, Y. *et al.* (2011) *In vitro* toxicity evaluation of graphene oxide on A549 cells. *Toxicol. Lett.* 200, 201–210
181 Jaworski, S. *et al.* (2013) In vitro evaluation of the effects of graphene platelets on glioblastoma multiforme cells. *Int. J. Nanomed.* 8, 413–420
182 Moore, T.L. *et al.* (2014) Systemic administration of polymer-coated nano-graphene to deliver drugs to glioblastoma. *Part. Part. Syst. Charact.* 31, 886–894
183 Corr, S.J. *et al.* (2013) Cytotoxicity and variant cellular internalization behavior of water-soluble sulfonated nanographene sheets in liver cancer cells. *Nanoscale Res. Lett.* 8, 208
184 Sasidharan, A. *et al.* (2011) Differential nano-bio interactions and toxicity effects of pristine versus functionalized graphene. *Nanoscale* 3, 2461–2464
185 Zhang, S.A. *et al.* (2011) In vitro and in vivo behaviors of dextran functionalized graphene. *Carbon* 49, 4040–4049
186 Chowdhury, S.M. *et al.* (2013) In vitro hematological and in vivo vasoactivity assessment of dextran functionalized graphene. *Sci. Rep.* 3 2584
187 Mu, Q. *et al.* (2012) Size-dependent cell uptake of protein-coated graphene oxide nanosheets. *ACS Appl. Mater Interfaces* 4, 2259–2266
188 Ali-Boucetta, H. *et al.* (2013) Purified graphene oxide dispersions lack in vitro cytotoxicity and in vivo pathogenicity. *Adv. Healthcare Mater.* 2, 433–441
189 Yang, K. *et al.* (2011) In vivo pharmacokinetics, long-term biodistribution, and toxicology of PEGylated graphene in mice. *ACS Nano* 5, 516–522
190 Duch, M.C. *et al.* (2011) Minimizing oxidation and stable nanoscale dispersion improves the biocompatibility of graphene in the lung. *Nano Lett.* 11, 5201–5207
191 Yan, L. *et al.* (2012) Can graphene oxide cause damage to eyesight? *Chem. Res. Toxicol.* 25, 1265–1270
192 Singh, S.K. *et al.* (2011) Thrombus inducing property of atomically thin graphene oxide sheets. *ACS Nano* 5, 4987–4996
193 Liao, K.-H. *et al.* (2011) Cytotoxicity of graphene oxide and graphene in human erythrocytes and skin fibroblasts. *ACS Appl. Mater Interfaces* 3, 2607–2615
194 Wang, K. *et al.* (2011) Biocompatibility of graphene oxide. *Nanoscale Res. Lett.* 6, 8
195 Yang, X. *et al.* (2014) Biocleavable graphene oxide based-nanohybrids synthesized via ATRP for gene/drug delivery. *Nanoscale* 6, 6141–6150
196 Patel, P.R.B. *et al.* (2016) Composite system of graphene oxide and polypeptide thermogel as an injectable 3D scaffold for adipogenic differentiation of tonsil-derived mesenchymal stem cells. *ACS Appl. Mater Interfaces* 8, 5160–5169
197 Imani, R. *et al.* (2015) Synthesis and characterization of an octaarginine functionalized graphene oxide nano-carrier for gene delivery applications. *Phys. Chem. Chem. Phys.* 17, 6328–6339

198 Zeng, Y. *et al.* (2015) Fast and facile preparation of PEGylated graphene from graphene oxide by lysosome targeting delivery of photosensitizer to efficiently enhance photodynamic therapy. *RSC Adv.* 5, 57725–57734
199 Tian, L. *et al.* (2014) Functionalized nanoscale graphene oxide for high efficient drug delivery of cisplatin. *J. Nanopart. Res.* 16, 2709
200 Pan, Y. *et al.* (2011) Water-soluble poly(N-isopropylacrylamide)-graphene sheets synthesized via click chemistry for drug delivery. *Adv. Funct. Mater.* 21, 2754–2763
201 Rana, V.K. *et al.* (2011) Synthesis and drug-delivery behavior of chitosan-functionalized graphene oxide hybrid nanosheets. *Macromol. Mater. Eng.* 296, 131–140
202 Fan, X. *et al.* (2013) The preparation and drug delivery of a graphene-carbon nanotube-Fe3O4 nanoparticle hybrid. *J. Mater. Chem. B* 1, 2658–2664
203 Zhou, L. *et al.* (2011) Graphene oxide noncovalent photosensitizer and its anticancer activity *in vitro*. *Chem. Eur. J.* 17, 12084–12091